Journal of Magnetic Resonance **154,** 196–204 (2002)
doi:10.1006/jmre.2001.2471, available online at http://www.idealibrary.com on IDEAL®

Efficient Triple-Quantum Excitation in Modified RIACT MQMAS NMR for $I = 3/2$ Nuclei

Kwang Hun Lim,* Thibault Charpentier,† and Alexander Pines*,[1]

*Materials Sciences Division, Lawrence Berkeley National Laboratory and Department of Chemistry, University of California at Berkeley, Berkeley, California 94720; and †Service de Chimie Moleculaire, CEA Saclay, 91191 Gif-sur-Yvette Cedex, France

Received April 19, 2001; revised October 24, 2001; published online January 16, 2002

A new approach involving the creation of triple-quantum (TQ) coherences from both TQ and central transitions (CT) is investigated, in order to enhance the efficiency of triple-quantum excitation for $I = 3/2$ nuclei. The RIACT excitation scheme, a soft $\pi/2$ and hard spin-locking pulse, is shown to induce both adiabatic coherence transfer between CT and TQ coherences and TQ nutation. By combining the RIACT scheme with the presaturation of the satellite transitions, a significant improvement in the TQ excitation can be achieved mainly through enhanced CT polarization via the RIACT mechanism, in particular for nuclei with moderate to large quadrupole coupling constants ($\geq$2.0 MHz). There also exists a nontrivial contribution from the TQ transition, which depends on the size of the quadrupole interaction. © 2002 Elsevier Science (USA)

INTRODUCTION

Multiple-quantum magic-angle spinning (MQMAS) spectroscopy, which effectively removes the second-order quadrupole interactions of half odd-integer quadrupole nuclei (*1, 2*), has been widely used for structural analysis of various inorganic materials such as zeolites, glasses, and ceramics (*3–10*). Two essential steps in the MQMAS experiments involve the creation of multiple-quantum (MQ) coherence and its subsequent conversion to central transition (CT) coherence. Both steps tend to be somewhat inefficient and also strongly dependent on the magnitude of the quadrupole interaction. It is also known that faster spinning of the sample, which is required for nuclei with large quadrupole coupling constants, degrades the MQ excitation efficiency (*11*). Sensitivity improvement in the MQ excitation and its conversion efficiency for large quadrupole interactions is, therefore, desirable for the study of inorganic compounds containing nuclei with large quadrupole coupling constants, for example ^{23}Na in zeolites NaX and NaY (5–6 MHz) (*12*) and ^{27}Al in dehydrated H-form zeolites (11–16 MHz) (*13*). Recently, a significant improvement in the conversion efficiency, in particular for large quadrupole interactions, was obtained by employing amplitude modulated (AM) pulses (*14–16*). Efforts have also been made to improve the MQ excitation efficiency (*17–20*) and recently, the interesting spin dynamics of quadrupole nuclei under, or near to, rotational resonance were exploited to enhance the sensitivity of MQMAS experiments, in particular for the MQ excitation experiment for $I = 3/2$ nuclei (*21*). The rotational resonance effect becomes more pronounced under more rapid sample rotation, resulting in superior sensitivity under faster MAS conditions, despite the fact that the rotational resonance phenomena are very sensitive to the offset and second-order quadrupole interaction due to small triple quantum (TQ) nutation frequency (*22*). It was demonstrated that a significant enhancement can be achieved over the standard two-pulse technique for $I = 3/2$ nuclei (^{87}Rb) with a moderately large quadrupole coupling constant of 3.2 MHz at a spinning speed of 30 kHz, using a 2.5 mm probe that has a relatively small rf inhomogeneity. The question remains whether improvements are possible in MQMAS under MAS speeds of 10–20 kHz, for which larger samples can be accommodated as well as the necessary requirements for large quadrupole interactions.

A straightforward method for MQ excitation is the application of a high power single radio-frequency (rf) pulse, which causes MQ coherences to nutate along the direction of the pulse (*23, 24*). An adiabatic coherence transfer between MQ and CT coherences induced by sample rotation (*25, 26*) was also used to generate MQ coherences, a method termed RIACT (rotationally induced adiabatic coherence transfer) (*18*). It is interesting to note that MQ coherences are mostly created from the MQ z-magnetization components in the conventional single pulse method, while the CT coherences are used to produce MQ coherences in the RIACT method. It may, therefore, be possible to increase the sensitivity of the MQ excitation by exploiting both mechanisms. If a soft solid $\pi/2$ pulse, which creates only CT coherences, is followed by a subsequent high power spin-locking pulse, then MQ coherences can be created from both the CT coherences via the adiabatic coherence transfer and from the MQ z-magnetization. This method can also be combined with a recently proposed method (*27*) which increases the central transition polarization by saturating satellite transitions, in order to further exploit the RIACT mechanism such an approach is advantageous, because the RIACT method was shown to be less

[1] To whom correspondence should be addressed. Fax: 510-486-5744. E-mail: pines@cchem.berkeley.edu.

1090-7807/02 $35.00
© 2002 Elsevier Science (USA)
All rights reserved.

sensitive to the quadrupole interaction (*18, 28*), compared to the conventional single pulse method. The present pulse scheme is quite similar to that used in the previous RIACT experiment, in which the coherent pathways only from the CT to MQ coherences were taken into account (*18, 28, 29*).

In this report, we present the modified RIACT scheme which creates TQ coherences from both TQ z-magnetization and CT coherences with an appropriate phase cycling scheme for $I = 3/2$ nuclear spins. It is also shown that an additional improvement in the TQ excitation can be achieved by enhancing the central transition polarization with a presaturation of the satellite transitions using amplitude modulated composite pulses.

THEORETICAL BACKGROUND

In this section, mechanisms for the TQ excitation in the two methods will be briefly described using fictitious spin 1/2 operators. A more detailed discussion of the formalism can be found elsewhere (*23, 24*). For $I = 3/2$ nuclei under rf irradiation, the spin Hamiltonian in a high magnetic field can be written as

$$H = 3\Delta\omega I_z^{1-4} + \Delta\omega I_z^{2-3} + \omega_Q\left(I_z^{1-2} - I_z^{3-4}\right) + \sqrt{3}\omega_1\left(I_x^{1-2} + I_x^{3-4}\right) + 2\omega_1 I_x^{2-3}, \quad [1]$$

where ω_1 is the rf field strength and $\Delta\omega$ is the offset frequency.

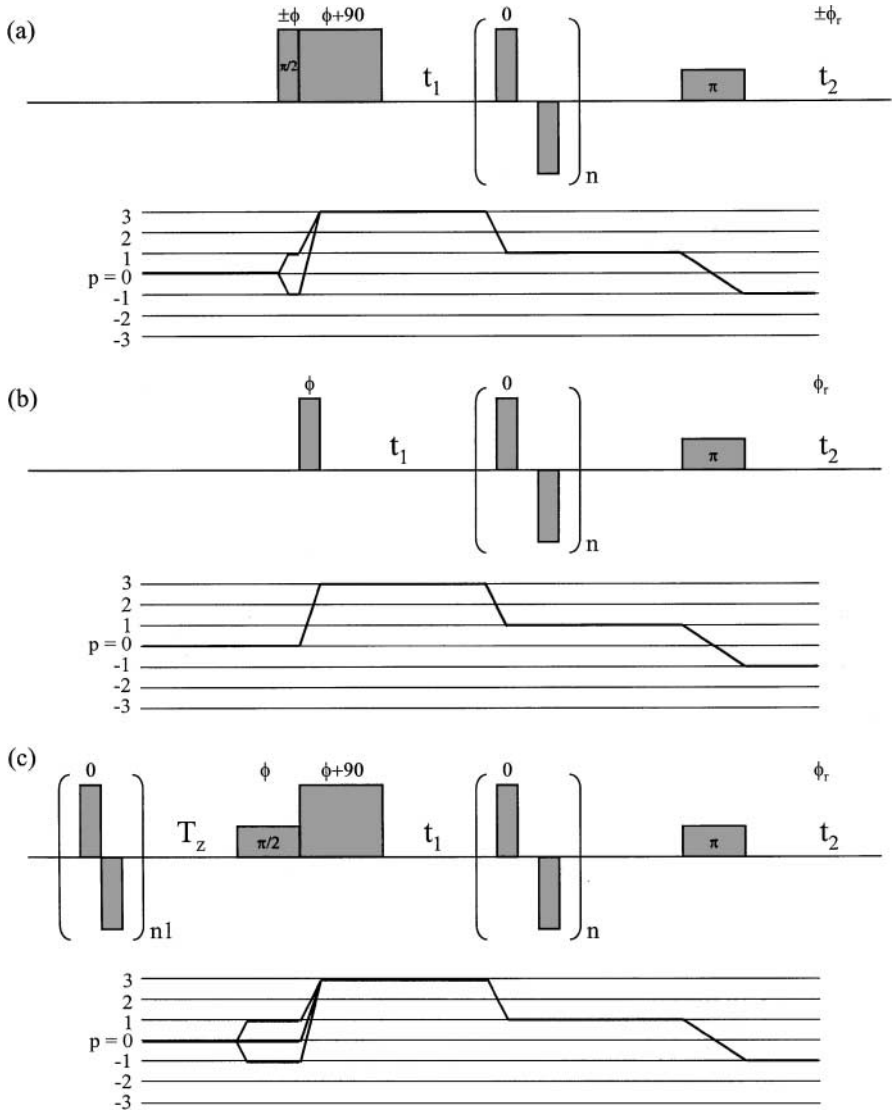

FIG. 1. Pulse sequences used in this study: (a) previous RIACT, (b) the conventional single pulse, and the (c) modified RIACT method, which exploits a combination of both (a) and (b). For 1D TQ-filtered NMR spectra, the echo coherence pathway drawn as a solid line is selected with the following phase cycling scheme: $\phi = 0°, 30°, 60°, 90°, 120°, 150°, 180°, 210°, 240°, 270°, 300°, 330°$; $\phi_r = 0°, 90°, 180°, 270°$. A CW rectangular pulse with pulse length of a quarter rotor period (RIACT pulse) was also used for the conversion pulse. For the presaturation of the satellite transitions shown in (c), composite $x\bar{x}$ pulses were applied for one rotor period and a delay (T_z) of 50 ms was used.

The first-order quadrupole frequency, ω_Q, is given by

$$\omega_Q = \frac{3e^2qQ}{2I(2I-1)\hbar}(3\cos^2\theta - 1 + \eta\sin^2\theta\cos 2\phi), \qquad [2]$$

where $(e^2qQ)/\hbar$ is the quadrupole coupling constant (C_Q) and η is the asymmetry parameter. The polar angles (θ, ϕ) describe the relative orientation of the quadrupole tensor, with the Zeeman field defining the z axis. For $\omega_Q \gg \omega_1$, the Hamiltonian, after suitable coordinate transformations, can be decomposed into commuting TQ (H^{1-4}) and CT (H^{2-3}) terms

$$H^{1-4} = \frac{3\omega_1^3}{2\omega_Q^2}I_x^{1-4} + 3\Delta\omega I_z^{1-4} \qquad [3]$$

$$H^{2-3} = 2\omega_1 I_x^{2-3} + \Delta\omega I_z^{2-3}. \qquad [4]$$

The initial equilibrium density operator (ρ_0) can also be written as the sum of TQ and CT z-magnetization terms

$$\rho_0 = 3I_z^{1-4} + I_z^{2-3}. \qquad [5]$$

Under the rf irradiation, the TQ and CT terms in the density operator will nutate within the TQ and the CT space, respectively, along the pulse direction (x axis). Thus, TQ coherence (I_y^{1-4}) can be generated under the influence of the single rf pulse only from the TQ z-magnetization (I_z^{1-4}) for $\omega_Q \gg \omega_1$, which is fulfilled for most crystallites under classical experimental conditions.

Under MAS, spin dynamics for quadrupolar nuclei become quite complicated due to the time dependence of the quadrupole interaction. However, optimum TQ coherence mostly occurs in short time ($<0.1\,\tau_r$; where τ_r is one rotor period), compared to the sample rotation period, so that the time dependence of ω_Q can be ignored. Under very fast MAS conditions, the assumption made above is no longer valid, and thus a more rigorous theoretical treatment is required. However, numerical simulations, which will be shown later, show that the TQ nutation behavior is not significantly changed during the short pulse length even under fast MAS conditions, but the efficiency is degraded due to the partially averaged out quadrupolar interaction (*11*).

On the other hand, external rf irradiation during MAS drastically changes the spin dynamics (in particular, spin-locking behavior of CT coherences) from what prevails for static samples. The sample rotation induces changes in the sign of $\omega_Q(t)$ (a zero-crossing of ω_Q), and the associated eigenvalues of the spin system. If the spinning is slow and ω_1 is sufficiently large, the central transition and multiple-quantum coherences are interconverted efficiently; such adiabatic passage has in fact been employed in the RIACT MQMAS experiments for $I = 3/2$ (*18*) and 5/2 nuclei (*29*), in order to create MQ coherences from the CT coherences. In the previous RIACT experiments, MQ coherences generated only from the CT coherences are taken into account in the phase cycling scheme, even though MQ z-magnetizations can also be converted to the MQ coherences via the MQ nutation during the spin-locking pulse. Thus, the application of a soft $\pi/2$ pulse, which creates only CT coherences while MQ z-magnetization remains intact, together with a hard spin-locking pulse, generates MQ coherences from both the CT coherence and MQ z-magnetization.

Figures 1a and 1b show the pulse scheme and corresponding coherence pathways for the previous RIACT and conventional single pulse methods. The pulse sequence used in the present study is depicted in Fig. 1c. In the modified RIACT scheme, the $\pi/2$ pulse is applied with very low rf power, and the $\pi/2$ and spin-locking pulse are treated as a composite pulse in the phase cycling scheme. In the new pulse sequence in Fig. 1c, composite $x\bar{x}$ pulses were also applied for one rotor period, prior to the MQMAS sequence, in order to saturate the satellite transitions, thereby, enhancing the CT polarization.

EXPERIMENTAL

Anhydrous Na_2HPO_4, $Na_2C_2O_4$, and Rb_2SO_4 (Aldrich) were used without further purification for the MQMAS experiments.

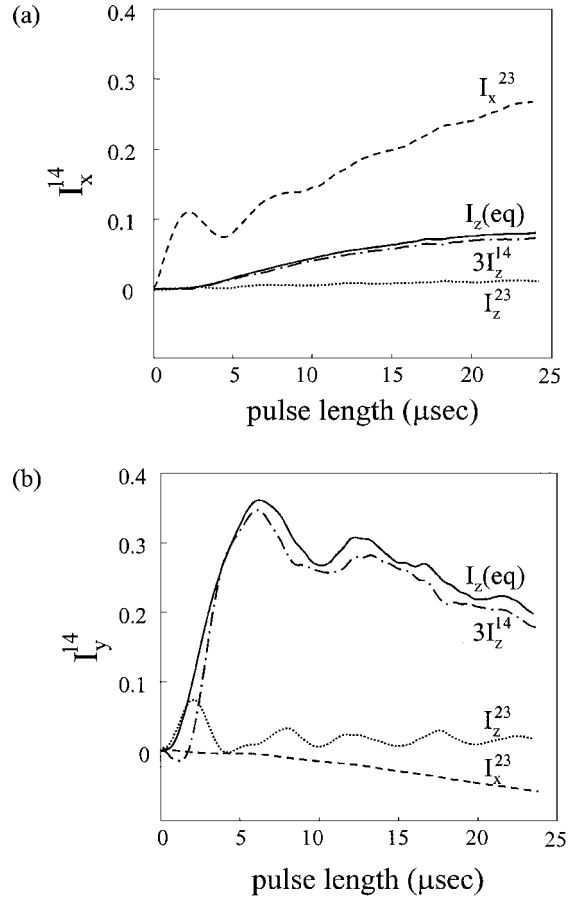

FIG. 2. Calculated eigenvalues of the TQ coherences of (a) I_x^{1-4} and (b) I_y^{1-4} under rf irradiation along the x direction applied to various initial density operators, as a function of the pulse length. A spinning speed (ω_r) of 10 kHz and rf field strength (ω_1) of 100 kHz were assumed for the calculations. A total of 1154 crystallite orientations were employed for the powder average.

All NMR spectra were acquired with Chemagnetics probes, on a Varian CMX Infinity 500 spectrometer where the resonance frequencies for ^{23}Na and ^{87}Rb are 132.2 and 163.6 MHz, respectively. The MQMAS NMR spectra acquired with fast MAS (>15 kHz) were obtained with a 3.2 mm probe, while other NMR spectra were obtained using a 4 mm probe with a spinning speed of 10 kHz. A rf field strength of 80–100 kHz for the hard pulses and acquisition delay of 1–15 s were used for the experiments. For the TQ excitation of Fig. 1b, the optimal pulse length was 5–5.8 μs, and 6.9 μs was the duration of the soft $\pi/2$ pulse. The number of AM pulse cycle for the TQ $\rightarrow$ CT conversion pulse was 3–5 with a pulse length of 1 μs and a time interval of 1 μs between the pulses. All the presaturation pulses were applied during one rotor period.

RESULTS AND DISCUSSION

Numerical simulations were performed to investigate how much gain in sensitivity of TQ excitations for ^{23}Na ($I = 3/2$) can be achieved by exploiting the two mechanisms. Figure 2 shows calculated expectation values of TQ coherences (I_x^{1-4}: (a), I_y^{1-4}: (b)) under the action of the rf irradiation along the x direction on various initial density operators, as a function of the pulse length. The quadrupole parameter ($C_Q = 2.4$ MHz;

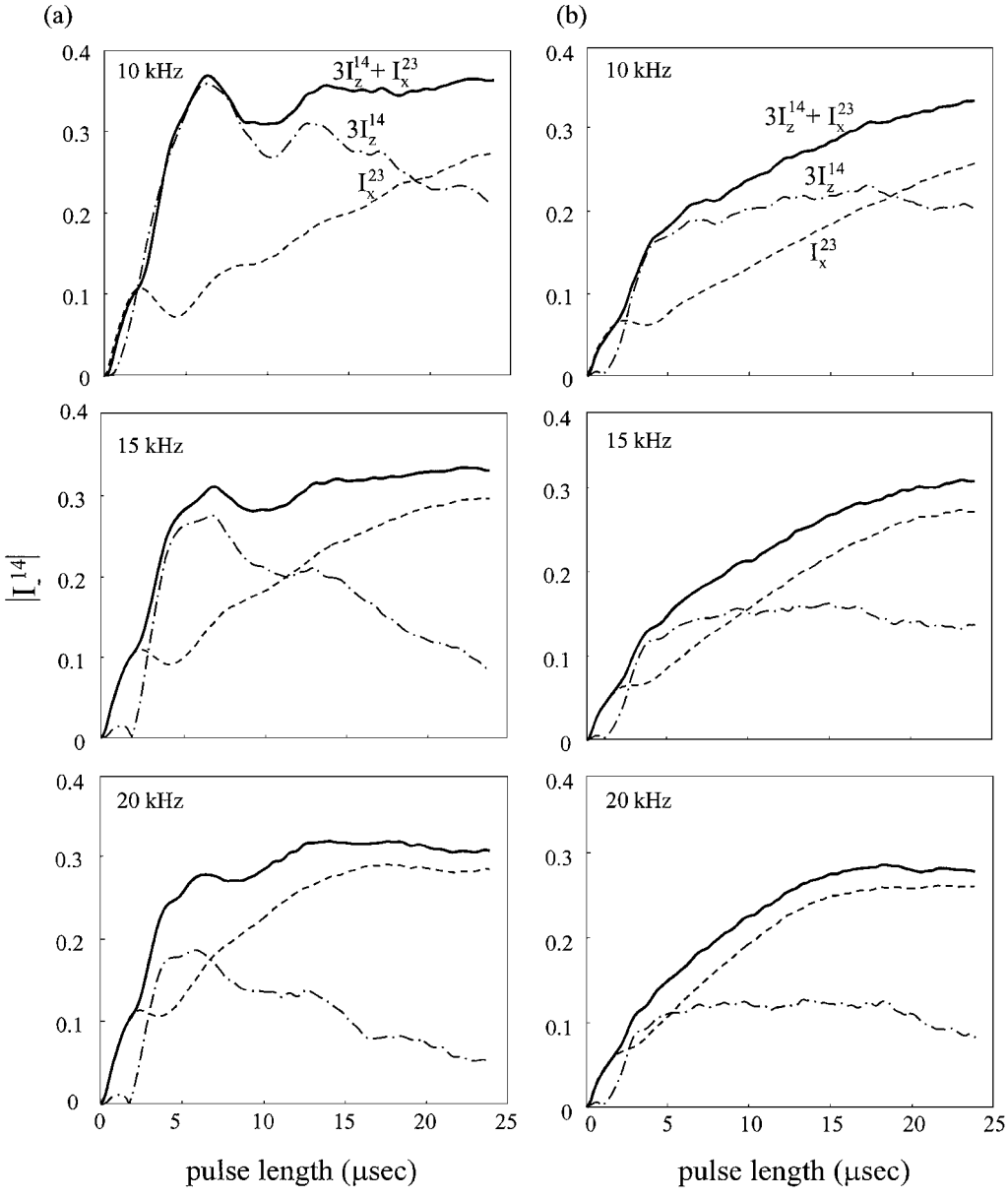

FIG. 3. Calculated TQ coherences of I_-^{1-4} induced from three initial density operators by single pulse irradiation for two quadrupole parameters: (a) C_Q of 2.4 MHz and $\eta = 0.77$ and (b) C_Q of 3.8 MHz and $\eta = 0.3$. Values of $\omega_r/2\pi$ =10 kHz and $\omega_1/2\pi = 100$ kHz were used for the calculations.

$\eta = 0.77$) used in this calculation corresponds to the value for the sodium in $Na_2C_2O_4$. As can be seen in Fig. 2b, most TQ coherences induced by the TQ nutation are generated from the TQ z-magnetization (I_z^{1-4}). As anticipated in the theory section, only the y component is generated, while the x component is induced by the second-order quadrupole interaction (see Fig. 2a). On the other hand, I_x^{1-4} can be efficiently created from the CT coherences induced by the adiabatic coherence transfer, while the intensity of I_y^{1-4} from the CT coherences also increases with time due to the second-order quadrupole interaction. The TQ coherences induced by the second-order quadrupole interaction can interfere with those derived from the primary mechanisms, and may result in a distortion of the anisotropic lineshape of the MQMAS spectrum.

Figure 3 shows calculated expectation values of TQ coherences (I_-^{1-4}) under the influence of a single rf pulse along the x direction on three initial density operators, at different spinning speeds (ω_r) and for two quadrupole parameters. The quadrupole coupling constant (C_Q) of 3.8 MHz used in Fig. 3b corresponds to the largest value for the sodium sites in Na_2HPO_4. The optimum TQ coherences from the MQ z-magnetization (I_z^{1-4}) induced by the nutation mechanism continuously decreases as the spinning speed increases, and the efficiency of the TQ excitation for the larger value of C_Q (3.8 MHz) in Fig. 3b is only half of that for the smaller value of C_Q (2.4 MHz). On the other hand, the optimum expectation value of the TQ coherences in the modified RIACT scheme does not change significantly with the spinning speed and with quadrupole interactions. In particular, the efficiency of the TQ excitation induced by the new scheme exceeds that of the single pulse excitation method for the large quadrupole interaction under fast MAS conditions, as can be seen in Fig. 3b. The new scheme is also expected to provide better sensitivity than the previous RIACT due to the contribution from TQ transitions, the gain in the sensitivity depending on the quadrupole interaction and spinning speed. However, the efficiency of the solid $\pi/2$ pulse that creates CT coherences (I_x^{2-3}) is dependent on the quadruple interaction, which depends on molecular orientation, so that all the crystallites in the powder cannot be excited simultaneously with the $\pi/2$ pulse. This indicates that the TQ signals from the CT transition via the RIACT mechanism will be slightly lower (80–90%) than the calculated values. In order to minimize the loss of the signals, low rf power should be used for the $\pi/2$ pulse.

The one-dimensional TQ-filtered NMR spectra of $Na_2C_2O_4$ obtained from the three different initial operators were observed experimentally as a function of the excitation pulse length (while $\pi/2$ pulse length is fixed), and are shown in Fig. 4. The first two TQ-filtered NMR spectra in Fig. 4a were obtained by the RIACT and the single pulse methods (in Figs. 1a and 1b), and the lower spectra were acquired with the modified RIACT method shown in Fig. 1c *without* presaturating satellite transitions. The experimental results shown in Fig. 4a were obtained by using a rectangular pulse with $\tau_r/4$ pulse length (RIACT pulse) as the conversion pulse at a spinning speed of 10 kHz. The changes in the intensity shown in Fig. 4a are consistent with those shown in the numerical calculations (see Fig. 3a). The lineshape distortions obtained by the RIACT and conventional methods are caused by the second-order quadrupole interaction; the distortions occur in a different way in the two cases because the second-order interactions affect the TQ coherences differently, as shown in

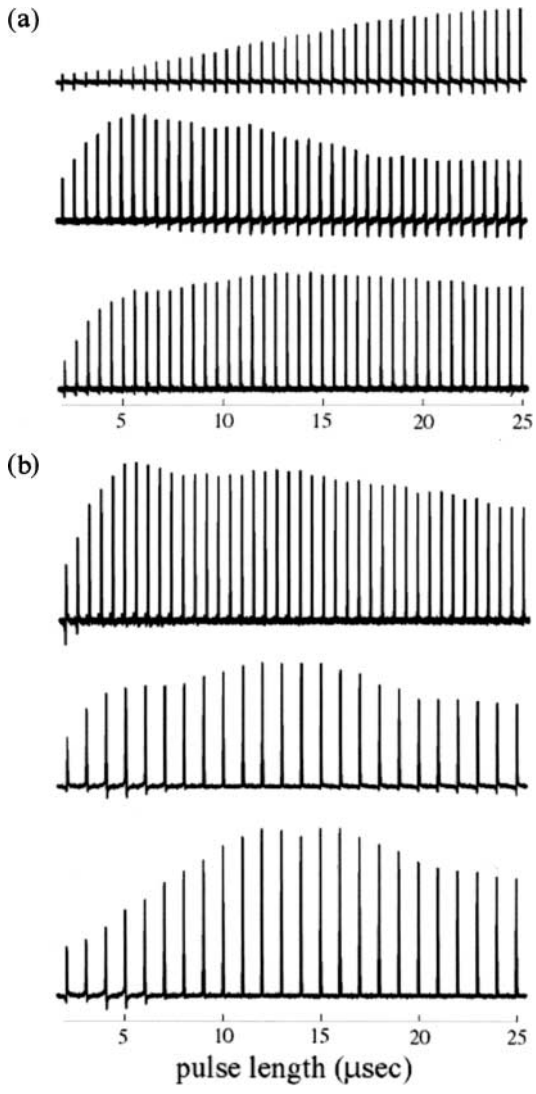

FIG. 4. Experimental TQ-filtered ^{23}Na 1D NMR spectra of $Na_2C_2O_4$ as a function of the excitation pulse length with a $\omega_r/2\pi = 10$ kHz and $\omega_1/2\pi = 100$ kHz. (a) The first two profiles were obtained with the RIACT and conventional single pulse method, and the lower one was acquired with the modified RIACT method shown in Fig. 1(c). The RIACT pulse was used for the conversion pulse and the presaturation AM pulses were *not* applied prior to the MQMAS experiments. (b) The experimental profiles were obtained with the new method, using composite $x\bar{x}$ pulses for conversion. The first two profiles were acquired at $\omega_r/2\pi = 10$ and 20 kHz, respectively, *without* applying presaturation pulses, while the lower one was obtained *with* a presaturation composite AM pulses, at $\omega_r/2\pi = 20$ kHz. The relative intensity of the profiles obtained at the two different spinning speeds cannot be compared, since the profiles were acquired with different probes.

Fig. 2. This destructive interference may result in a loss in the sensitivity and lineshape distortion. Optimum TQ coherence in the conventional method occurs in a very short time ($\sim$5 μs), while a quarter rotor period (25 μs) is the optimum pulse length in the RIACT method. Thus, the TQ intensity profile in the modified RIACT method is quite broad due to the overlap of the two profiles where optimum pulse lengths are quite different from each other. Efficiency of the TQ excitation is slightly improved in the new method, in comparison to both conventional methods. Under fast MAS conditions required for the large quadrupole interactions, the efficiency will improve further since $\tau_r/4$ which is the optimum pulse length for the RIACT method becomes shorter, and may result in more overlap between the two profiles.

Figure 4b shows the TQ-filtered spectra obtained with the new scheme at different spinning speeds by using amplitude modulated (AM) pulses for the conversion. The lower profile was obtained *with* a satellite presaturation pulse, at a spinning speed of 20 kHz, while the first two profiles were acquired at spinning speeds of 10 and 20 kHz, respectively, *without* satellite presaturation pulses. A gain of $\sim$1.4 in sensitivity was achieved by using AM pulses for the conversion pulse, over the sensitivity obtained with the RIACT pulse. Under 20 kHz MAS, the optimum TQ efficiency, which occurs at $\sim\tau_r/4$ (12 μs), is slightly improved, in comparison to the optimum value (at $\sim$5 μs)

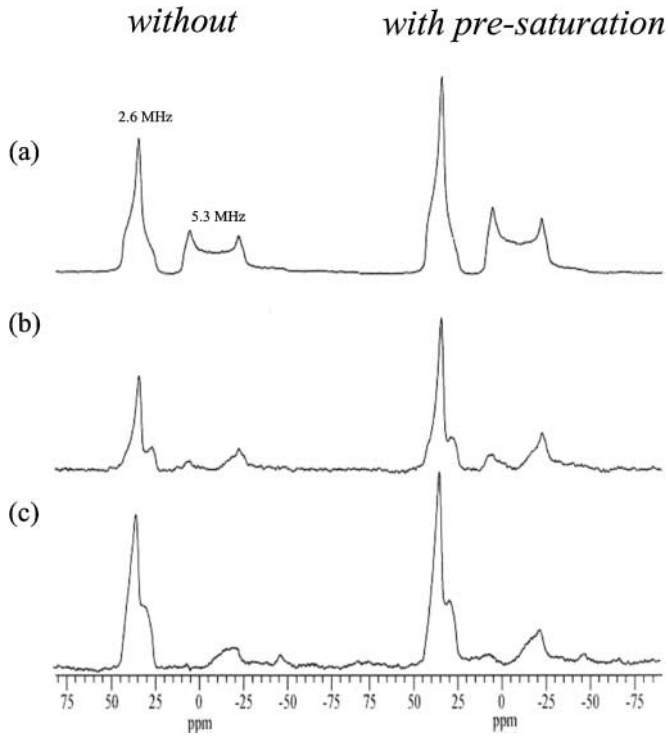

FIG. 5. Experimental ^{87}Rb 1D MAS (a) and TQ-filtered spectra of Rb_2SO_4 obtained with the (b) previous and (c) modified RIACT scheme at $\omega_r/2\pi =$ 16.8 kHz and $\omega_1/2\pi = 100$ kHz. Presaturation pulses of 0.6 μs were applied for one rotor period.

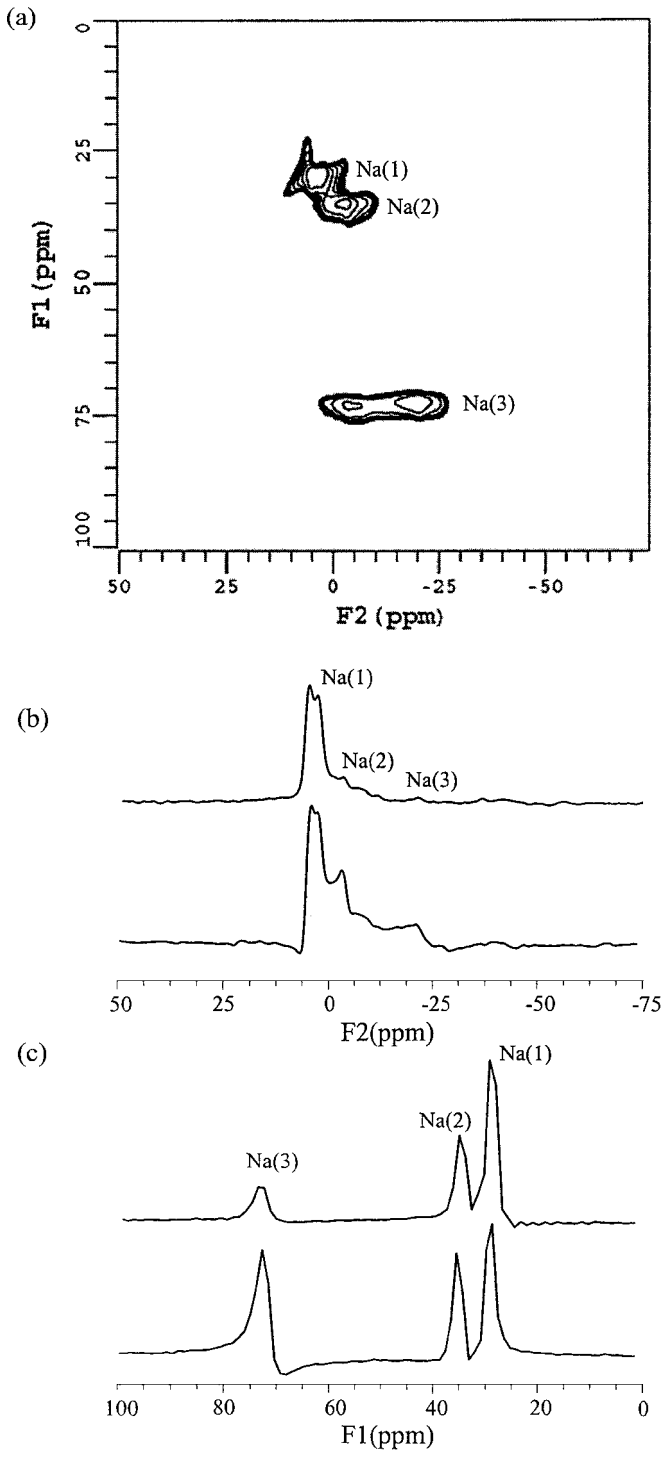

FIG. 6. Two-dimensional ^{23}Na MQMAS spectrum (a) of anhydrous Na_2HPO_4 and projection spectra onto the (b) anisotropic and (c) isotropic dimensions. The lower projection spectra were obtained with the new method and the other spectra were acquired with the conventional method. A hypercomplex 512×128 data set was acquired at $\omega_1/2\pi = 80$ kHz and $\omega_r/2\pi = 16.8$ kHz, and 36 FIDs were collected for each t_1 increment of 25.7 μs with an acquisition delay of 5 s. A pulse length of a quarter rotor period (15 μs) was used for the excitation pulse in the new scheme. FAM pulses were employed for the TQ $\rightarrow$ SQ conversion.

obtained by the conventional single pulse method. Since a considerable amount of the TQ signals generated at $\sim\tau_r/4$ are induced by the RIACT mechanism (see Fig. 3), an additional improvement can be achieved by enhancing the central transition polarization through saturation of the satellite transitions. In the lower profile of Fig. 4b acquired by the modified RIACT method at a spinning speed of 20 kHz *with* presaturation of the satellite transitions, a factor of 1.4 enhancement in the MQ excitation was achieved, in comparison to the optimum TQ excitation obtained *without* the presaturation pulses. The pulse length of 0.8 μs was used to enhance the CT polarization, which resulted in a factor of 1.5 enhancement in the 1D MAS experiment. It is important to note that the enhancement of the CT polarization is achieved by sacrificing the polarization of the TQ polarization, so that a contribution from the TQ *z*-magnetization to TQ coherences will be lowered if the presaturation pulses are applied prior to the MQMAS experiment (*30*).

In order to check contributions from the TQ transition for the TQ excitation in the modified RIACT scheme, 1D TQ-filtered spectra were acquired using the modified and previous RIACT scheme, with and without applying presaturation pulses. Figure 5 shows ^{87}Rb 1D MAS spectra of Rb_2SO_4 (a), and the TQ-filtered spectra obtained with the (b) previous and (c) modified RIACT scheme. The spectra on the right side were obtained by applying the presaturation pulses of 0.6 μs during one rotor period. In the left-side spectra in Figs. 5b and 5c, the new scheme demonstrates improved sensitivity over the previous RIACT scheme for the ^{87}Rb with C_Q of 2.6 MHz, indicating that there exists a significant amount of contribution from the TQ-*z* magnetization. By applying the presaturation pulses, overall efficiencies for the 1D MAS and the both MQMAS schemes are enhanced, the improvement in the new scheme being less prominent than in the previous RIACT scheme due to the reduced TQ-*z* magnetization (*30*). However, a substantial amount of contribution from TQ transition is still observed even with the reduced TQ polarization for the smaller C_Q of 2.6 MHz, as can be inferred from Figs. 5b and 5c. For the larger value of C_Q of 5.3 MHz, no significant changes in the lineshapes and intensities were observed, indicating that the central transition mainly contributes to the generation of the TQ coherences for the large quadrupole interaction.

Finally, two-dimensional MQMAS experiments were performed on anhydrous Na_2HPO_4 and Rb_2SO_4, to investigate how much enhancement can be achieved by exploiting the two mechanisms *with* the enhanced CT polarization, compared with the conventional single pulse method. Figure 6 shows the ^{23}Na 2D MQMAS spectrum obtained *without* using shifted-echo method (a), and projection spectra onto the anisotropic (F2) and isotropic (F1) dimensions in (b) and (c), respectively. The top projection spectra in Figs. 5b and 5c were obtained with the conventional single pulse excitation scheme, while the lower spectra were obtained with the modified RIACT excitation scheme *with* presaturation of the satellite transitions. The lineshape in the projection spectra is significantly distorted, since only echo signal can

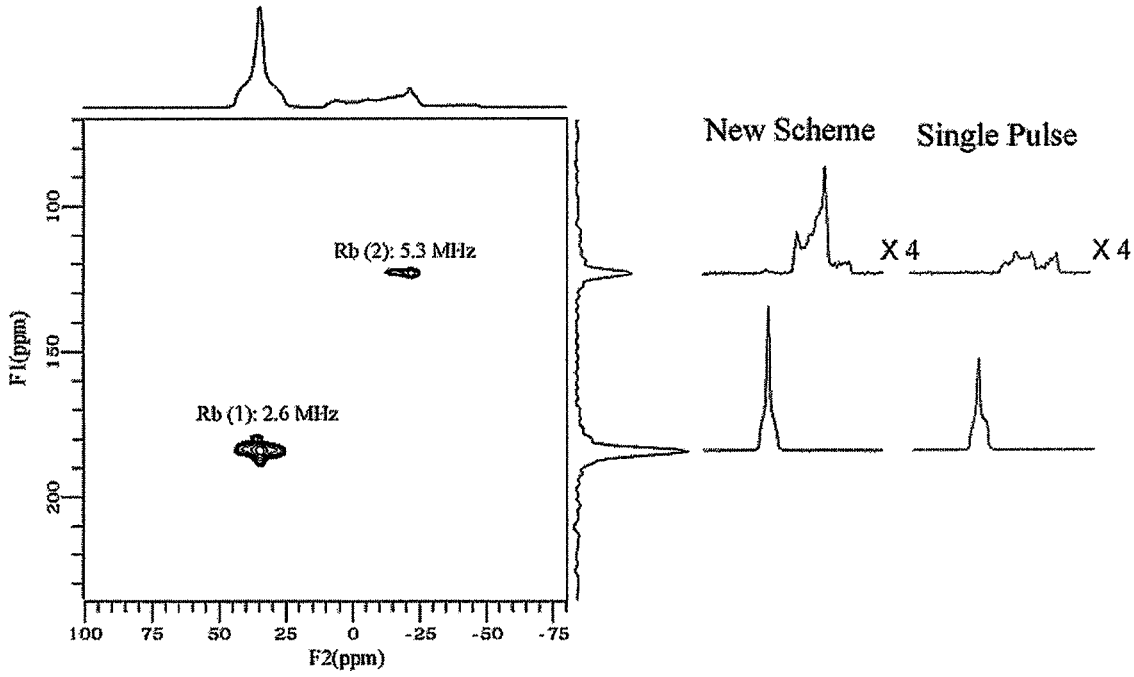

FIG. 7. Two-dimensional ^{23}Rb MQMAS spectrum of Rb_2SO_4 along with the slices obtained with the new scheme and the high power single pulse method. A hypercomplex 512 × 128 data set was acquired at $\omega_1/2\pi = 100$ kHz and $\omega_r/2\pi = 16.8$ kHz with the shifted echo method, and 36 FIDs were collected for each t_1 increment of 12.8 μs with an acquisition delay of 1 s. Presaturation pulses of 0.6 μs were applied during one rotor period and FAM pulses were used for the conversion.

be detected with FAM conversion pulses (*31*). For the Na(1) site with a small C_Q of 1.3 MHz, the efficiency of the new scheme was comparable to that of the conventional method. However, the new method was superior to the conventional method for the moderate C_Q of 2.0 MHz (Na(2)) and the large C_Q of 3.8 MHz (Na(3)), as can be seen in the projection spectra. The projection spectra also indicate that the new MQMAS method is less sensitive to the magnitude of the quadrupole interaction. Since the pulse length of the presaturation composite pulses depends on the magnitude of the quadrupole interaction, a uniform CT polarization enhancement could not be achieved for the three sites. A pulse length of 0.84 μs used in this study yielded an enhancement factor of $\sim$1.2 for Na(1), and $\sim$1.5 for Na(2) and Na(3).

Two-dimensional ^{87}Rb MQMAS spectrum of Rb_2SO_4 obtained *with* the shifted-echo method is shown in Fig. 7. Pure-absorption slices along with the 2D spectrum show that the modified RIACT MQMAS *with* the presaturation of the satellite transitions provides a better sensitivity compared to the single pulse excitation, in particular for the large value of C_Q (5.3 MHz). It is interesting to note that the lineshape for the ^{87}Rb with C_Q of 5.3 MHz is similar to that obtained with the RIACT excitation (*29*), suggesting that main TQ signals came from the CT polarization via the RIACT mechanism. However, little bumps between the two singularities are also shown, which appear to be generated from TQ-z magnetization via the nutation mechanism. For the smaller value of C_Q (2.6 MHz), the lineshape is more similar to that obtained with the single pulse excitation shown in the right side than the RIACT lineshape, as shown in Fig. 5b (*29*). These indicate that a nontrivial contribution from TQ transitions *does* exist even with a reduced polarization by the presaturation pulses, the amount of the contribution depending on the quadrupole interaction. A more systematic investigation is currently being carried out in order to quantify contributions from the CT and TQ transitions as a function of quadrupole interactions.

CONCLUSION

We have demonstrated that an enhancement of the triple quantum excitation for moderate and larger quadrupole interactions can be achieved by exploiting a combination of two previous MQ excitation mechanisms for $I = 3/2$ nuclei. The RIACT mechanism could be used to advantage by enhancing the central transition polarization through the application of composite $x\bar{x}$ pulses prior to the MQMAS experiments. Despite the fact that TQ polarization is reduced due to the presaturation pulses, the modified RIACT scheme still has an advantage over the previous RIACT scheme, owing to the contributions from TQ transitions. The new MQ excitation scheme is also less sensitive to the magnitude of the quadrupole interaction, and thus this method should be useful for the study of various materials that have a broad distribution of quadrupole interactions. Further investigations for higher spin systems are also underway.

ACKNOWLEDGMENTS

This work was supported by the Director, Office of Science, Office of Basic Energy Sciences, Materials Sciences Division, of the U.S. Department of Energy under Contract DE-AC03-76SF00098. The authors also thank P. J. Grandinetti and co-workers for providing a preprint of their FASTER MQMAS work.

REFERENCES

1. L. Frydman and J. S. Harwood, Isotropic spectra of half-integer quadrupolar spins from bidimensional magic-angle spinning NMR, *J. Am. Chem. Soc.* **117,** 5367–5368 (1995).
2. A. Medek, J. S. Harwood, and L. Frydman, Multiple-quantum magic-angle spinning NMR: A new method for the study of quadrupolar nuclei in solids, *J. Am. Chem. Soc.* **117,** 12779–12787 (1995).
3. S. Ganapathy, T. K. Das, R. Vetrivel, S. S. Ray, T. Sen, S. Sivasankr, L. Delevoye, C. Fernandez, and J.-P. Amoureux, Anisotropic chemical shielding, M-Site ordering, and characterization of extraframework cations in ETS-10 studied through MAS/MQ-MAS NMR and molecular modeling techniques, *J. Am. Chem. Soc.* **120,** 4752–4762 (1998).
4. K. H. Lim and C. P. Grey, Characterization of extra-framework cation positions in zeolites NaX and NaY with very fast ^{23}Na MAS and multiple quantum MAS NMR spectroscopy, *J. Am. Chem. Soc.* **122,** 9768–9780 (2000).
5. S. Wang and J. F. Stebbins, Multiple-quantum magic-angle spinning O-17 NMR studies of berate, borosilicate, and boroaluminate classes, *J. Am. Ceram. Soc.* **82,** 1519–1528 (1999).
6. S. J. Hwang, C. Fernandez, J.-P. Amoureux, J. W. Han, J. Cho, S. W. Martin, and M. Prusi, Structural study of $xNa_2S + (1 - x)B_2S_3$ glasses and polycrystals by multiple-quantum MAS NMR of ^{11}B and ^{23}Na, *J. Am. Chem. Soc.* **120,** 7337–7346 (1998).
7. J. F. Stebbins and Z. Xu, NMR evidence for excess non-bridging oxygen in an aluminosilicate glass, *Nature* **364,** 60–62 (1998).
8. J. H. Baltisberger, Z. Xu, J. F. Stebbins, S. H. wang, and A. Pines, Triple-quantum two-dimensional ^{27}Al magic-angle spinning nuclear magnetic resonance spectroscopic study of aluminosilicate and aluminate crystals and glasses, *J. Am. Chem. Soc.* **118,** 7209–7214 (1996).
9. P. Faucon, T. Charpentier, D. Bertrandie, A. Nonat, J. Virlet, and P. C. Petet, Characterization of calcium aluminate hydrates and related hydrates of cement pastes by ^{27}Al MQ-MAS NMR, *Inorg. Chem.* **37,** 3726–3733 (1998).
10. C. A. Fyfe, J. L. Bretherton, and L. Y. Lam, Detection of the 'invisible aluminium' and characterisation of the multiple aluminium environments in zeolite USY by high-field solid-state NMR, *Chem. Commun.* **131,** 1575–1576 (2000).
11. J.-P. Amoureux, M. Pruski, D. P. Lang, and C. Fernandez, The effect of RF power and spinning speed on MQMAS NMR, *J. Magn. Reson.* **131,** 170–175 (1998).
12. M. Feuerstein, M. Hunger, G. Engelhardt, and J.-P. Amoureux, Characterisation of sodium cations in dehydrated zeolite NaX by Na-23 NMR spectroscopy, *Solid State NMR* **7,** 95–103 (1996).
13. H. Ernst, D. Freude, and I. Wolf, In Zeolites and related microporous materials: State of the Art 1994, Studies in surface science and catalysis, in "Multinuclear NMR-studies of acid sites in zeolites" (J. Weitkamp, H. G. Karge, H. Pfeifer, and W. Holderich, Eds.), pp. 381–385, Elsevier: Amsterdam (1994).
14. P. K. Madhu, A. Goldbourt, L. Frydman, and S. Vega, Sensitivity enhancement of the MQMAS NMR experiment by fast amplitude modulation of the pulses, *Chem. Phys. Lett.* **307,** 41–47 (1999).

15. A. Goldbourt, P. K. Madhu, and S. Vega, Enhanced conversion of triple to single-quantum coherence in the triple-quantum MAS NMR spectrosocopy of spin-5/2 nuclei, *Chem. Phys. Lett.* **320,** 448–456 (2000).
16. T. Vosegaard, D. Massiot, and P. J. Grandinetti, Sensitivity enhancements in MQ-MAS NMR of spin-5/2 nuclei using modulated rf mixing pulses, *Chem. Phys. Lett.* **326,** 454–460 (2000).
17. C. Fernandez and J.-P. Amoureux, 2D Multiple-quantum MAS-NMR spectroscopy of ^{27}Al in aluminophosphate molecular-sieves, *Chem. Phys. Lett.* **242,** 449–454 (1995).
18. G. Wu, D. Rovnyank, and R. G. Griffin, Quantitative multiple-quantum magic-angle-spinning NMR spectroscopy of quadrupolar nuclei in solids, *J. Am. Chem. Soc.* **118,** 9326–9332 (1996).
19. S. Ding and C. A. McDowell, Shaped pulse excitation in multi-quantum magic-angle spinning spectroscopy of half-integer quadrupole spin systems, *Chem. Phys. Lett.* **270,** 81–86 (1997).
20. L. Marinelli, A. Medek, and L. Frydman, Composite pulse excitation schemes for MQMAS NMR of half-integer quadrupolar spins, *J. Magn. Reson.* **132,** 88–95 (1998).
21. T. Vosegaard, P. Florian, D. Massiot, and P. J. Grandinetti, Multiple quantum magic-angle spinning using rotary resonance excitation, *J. Chem. Phys.* **114,** 4618–4624 (2001).
22. J. D. Walls, K. H. Lim, and A. Pines, Theoretical studies of the spin-dynamics of quadrupolar nuclei at rotational resonance conditions, *J. Chem. Phys.*, accepted.
23. A. Wokaun and R. R. Ernst, Selective excitation and detection in multilevel spin systems-application of single transition operators, *J. Chem. Phys.* **67,** 1752–1758 (1977).
24. S. Vega, Fictitious spin-1/2 operator formalism for multiple quantum NMR, *J. Chem. Phys.* **68,** 5518–5527 (1978).
25. A. J. Vega, Cross polarization of half-integer spins in rotating samples, *Solid State Nucl. Magn. Reson.* **1,** 17 (1992).
26. A. J. Vega, MAS NMR spin locking of half–integer quadrupolar nuclei, *J. Magn. Reson.* **96,** 50–68 (1992).
27. Z. Yao, H. T. Kwak, D. Sakellariou, L. Emsley, and P. J. Grandinetti, Sensitivity enhancement of the central transition NMR signal of quadrupolar nuclei under magic-angle spinning, *Chem. Phys. Lett.* **327,** 85–90 (2000).
28. K. H. Lim and C. P. Grey, Analysis of the anisotropic dimension in the RIACT (II) Multiple Quantum MAS NMR experiment for $I = 3/2$ nuclei, *Solid State Nucl. Magn. Reson.* **13,** 101–112 (1998).
29. T. Mildner, M. E. Smith, and R. Dupree, 2D five quantum MAS NMR using rotationally induced coherence transfer, *Chem. Phys. Lett.* **306,** 297–302 (1999).
30. H. T. Kwak, S. Prasad, Z. Yao, P. J. Grandinetti, J. R. Sachleben, and L. Emsley, Enhanced sensitivity in RIACT/MQ-MAS NMR experiments using rotor assisted population transfer, *J. Magn. Reson.* **150,** 71–80 (2001).
31. T. Vosegaard, P. Florian, P. J. Grandinetti, D. Massiot, Pure absorption-mode spectra using a modulated RF mixing period in MQMAS experiments, *J. Magn. Reson.* **143,** 217–222 (2000).